Design of Taper Structure for Highly Efficient Coupling Between 1-D Photonic Crystal Coupled Resonator Optical Waveguide and Straight Waveguide

Yuki Kawaguchi, Kunimasa Saitoh, *Member, IEEE*, and Masanori Koshiba, *Fellow, IEEE*

***Abstract*—This paper presents a design method of a taper structure for highly efficient coupling between 1-D photonic crystal coupled resonator optical waveguides (1-D PC-CROWs) and input straight waveguides. We propose a new taper structure where not only air hole radius but also waveguide width are varied linearly in order to adjust the dispersion curves shift. By using the proposed tapered structure, we can connect each waveguide with high transmission over wide bandwidth. Our numerical simulation results show that a transmission of 98% around 1550 nm wavelength in a 6.6 μm long taper can be obtained with a 42 nm bandwidth.**

***Index Terms*—Coupled resonator optical waveguide (CROW), finite-element method (FEM), photonic crystal.**

I. Introduction

COUPLED RESONATOR OPTICAL WAVEGUIDEs (CROWs) are highly attractive for integrated delay lines, nonlinear effects enhancement [1], and dispersion compensators [2]. Especially, optical delay lines have emerged as key components for future optical networks and information processing systems. There is a wide range of applications of optical delay lines, such as optical packet switches [3], [4], optical buffers [5], optical regenerators [6], wavelength converters [7], and optical delay-line filters [8]. CROWs are attractive for these applications because of their specific small group velocity and zero group velocity dispersion (GVD) at the transmission miniband [9]–[19]. CROWs can be classified in several categories in terms of the resonance structures such as, CROWs relying on ring resonators [18], Fabry-Perot cavities, and photonic crystal (PC) microcavities [12], [13], [15], [16], [20]. Among configurations relying on one- to three-dimensional PC cavities, 1-D PC-CROWs based on photonic wires are the most attractive in terms of simplicity, while keeping the advantages of PCs such as compactness and integrability [21], [22]. One of the drawbacks of 1-D PC-CROWs is its intrinsic propagation losses due to diffraction. This strongly limits their usefulness in various applications [23]. However, recently we have shown a loss reduction mechanism for the 1-D PC-CROWs and low-loss 1-D PC-CROWs structure for the first time to the best of our knowledge [24], therefore the low-diffraction-loss 1-D PC-CROWs can be a good candidate for developing various ultra compact optical circuits. When we construct optical devices based on PC-CROWs, it is necessary to efficiently couple the light into CROWs from regular waveguides with low reflection over wide wavelength range. Zain *et al.* proposed a taper structure to achieve high efficiency coupling between straight waveguides and single defect high-Q nanocavity [25]. However, the proposed taper can connect each waveguide only at a resonance wavelength. In this paper, we present a design method of a taper structure for highly efficient and broad band connection between 1-D PC-CROWs and input straight waveguides.

The remainder of this paper is structured as follows. In Section II, we first describe a model of 1-D PC-CROWs and the need of a taper structure by considering the transmission characteristic of directly coupled CROWs and straight waveguides. Next, we show a design method of a taper structure, where the tapering is achieved by a linear variation in the air-hole radius. We further examine the dispersion relationship for varied air hole radius and propose another tapered structure where the air hole radius and the waveguide width are varied simultaneously. In Section III, the effect of waveguide parameters that construct the taper is investigated and miniaturized taper structure is also shown. In Section IV, fabrication tolerances are discussed. In Section V, we summarize our work.

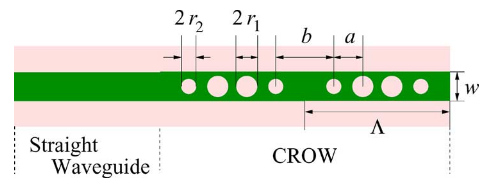

Fig. 1. Top view of 1-D PC-CROW directly connected to input straight waveguide (type 1).

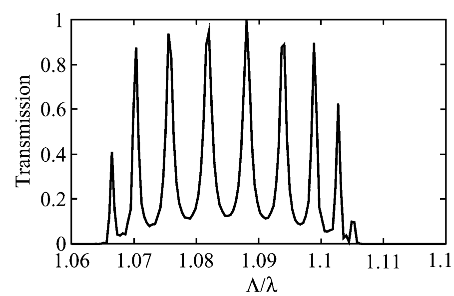

Fig. 2. Transmission characteristics for a type-1 tapered structure.

Manuscript received October 15, 2008; revised February 09, 2009. Current version published July 09, 2009. The work of Y. Kawaguchi was supported by the Japan Society for the Promotion of Science.

The authors are with the Graduate School of Information Science and Technology, Hokkaido University, Sapporo 060-0814, Japan (e-mail: kawaguchi@icp.ist.hokudai.ac.jp; ksaitoh@ist.hokudai.ac.jp; koshiba@ist.hokudai.ac.jp).

Color versions of one or more of the figures in this paper are available online at http://ieeexplore.ieee.org.

Digital Object Identifier 10.1109/JLT.2009.2019734

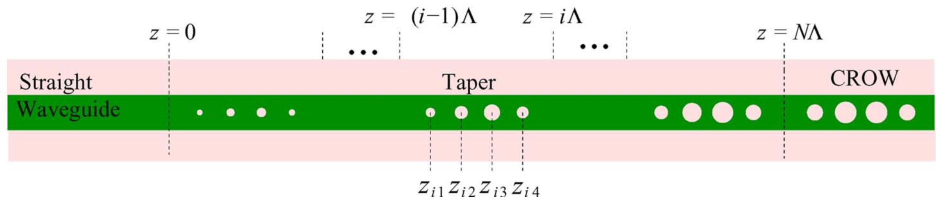

Fig. 3. Connection between 1-D PC-CROW and input straight waveguide using type-2 tapered structure, where the waveguide width is kept constant in the taper region.

II. Design Method of Taper Structures

A. Direct Connection Between CROWs and Straight Waveguides

We consider a 1-D PC-CROW structure which is connected with straight waveguide as shown in Fig. 1. We set structural parameters of CROWs as follows. The lattice constant a of 1-D PCs is 300 nm, the waveguide width w is $1.2a = 360$ nm, and the air hole radius r_1 is $0.3a = 90$ nm. We set the defect after every fourth air hole to make resonance structure, the cavity distance is set as $b = 2.5a = 750$ nm, and the intercavity distance Λ is $5.5a = 1650$ nm in the present case. We use silicon, with the refractive index of 3.48, as the core material and air as the cladding material. We assume that there is no variation in the y-direction. To reduce the diffraction losses, we set the radius of the air hole "adjacent" to the cavity as $r_2 = 0.2a = 60$ nm for minimizing the reflection at the cavity edge [24]. The tangential wavenumber components of the leaky guided modes which couple to cladding modes can be decreased, resulting in the reduction of propagation losses due to diffraction. The propagation losses of this 1-D PC-CROW is ~0.2 dB/mm [24]. Note that, the scattering loss in y-direction is not considered in this case, therefore the propagation losses of a real 1-D PC-CROW may be larger.

At first, we consider a direct connection between ten periods of the CROWs and the straight waveguide (type 1). Fig. 2 shows the transmission characteristic for the TM mode calculated by 2-D finite-element time domain beam propagation method (FETD-BPM) [26], where the magnetic field is polarized along y-axis. We can see from this figure that we cannot achieve high transmission over wide bandwidth due to the effect of reflection at the connection interface, even though there are some high transmission peaks. Therefore, we should design a taper structure to connect each waveguides with a high transmission.

B. Tapering Connection Between CROWs and Straight Waveguides

To improve the transmission characteristics, the CROW and the straight waveguide are connected by the taper structure as shown in Fig. 3 (type 2), where N is the number of periods that constructs the taper region, namely, total length of the taper becomes $N\Lambda$. The starting position of the waveguide taper is assumed to be $z = 0$ and the center position of jth ($j = 1, 2, 3, 4$) air hole at ith ($i = 1, 2, \ldots, N$) fundamental structure is defined as $z = z_{ij}$. To make the gentle variation of the refractive index along the propagation direction, we vary the air hole radius linearly as

$$R_{ij} = R_0 + (1 - R_0)/(N\Lambda) \tag{1}$$

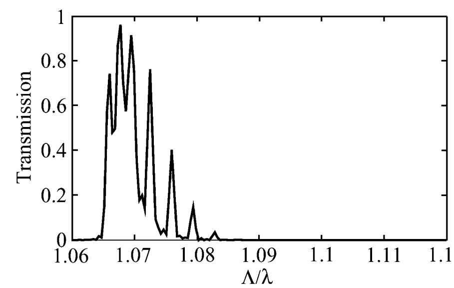

Fig. 4. Transmission characteristics for a type-2 tapered structure.

where R_{ij} and R_0 are the reduction rate of the air hole radius at $z = z_{ij}$ and $z = 0$, respectively. The air hole radius at $z = z_{ij}$ becomes $r_1 R_{ij}$ (for $j = 2, 3$) or $r_2 R_{ij}$ (for $j = 1, 4$). We can see from (1) that the air hole radius at the tapered waveguide is determined by setting N and R_0. We further show how to calculate the air hole radius in the tapered section with $N = 9$ and $R_0 = 0.1$ structure. For example, we consider the ninth ($i = 9$) fundamental structure. The center position of the air hole: z_{91}, z_{92}, z_{93}, and z_{94} are

$$\begin{aligned} z_{91} &= 8\Lambda + \frac{1}{2}b = 45.25a \\ z_{92} &= z_{91} + a = 46.25a \\ z_{93} &= z_{92} + a = 47.25a \\ z_{94} &= z_{93} + a = 48.25a. \end{aligned} \tag{2}$$

By assigning these values to (1), the air hole radius in this segment is determined as follows:

$$\begin{aligned} r_{91} &= r_2 R_{91} = 0.92 r_2 = 55 \text{ nm} \\ r_{92} &= r_1 R_{92} = 0.94 r_1 = 85 \text{ nm} \\ r_{93} &= r_1 R_{93} = 0.96 r_1 = 86 \text{ nm} \\ r_{94} &= r_2 R_{94} = 0.98 r_2 = 59 \text{ nm}. \end{aligned}$$

Fig. 4 shows the transmission characteristic for the CROW using a type-2 tapered structure with $N = 9$ and $R_0 = 0.1$. The transmission is limited to the lower frequency range and it is highly oscillating. In addition, we can see from this figure that the transmission at higher frequency range is completely suppressed even if we use taper structure for air hole radius variation.

To understand the transmission suppression at higher frequency range, the dispersion curves for CROWs with different air-hole radius are plotted in Fig. 5(a), where the air hole radii r_1 and r_2 are changed to r_1' and r_2', respectively, at a fixed waveguide width $w = 1.2a$. The dispersion curve of a straight waveguide is also plotted in Fig. 5(a) in order to make a comparison. We can see from these results that the dispersion

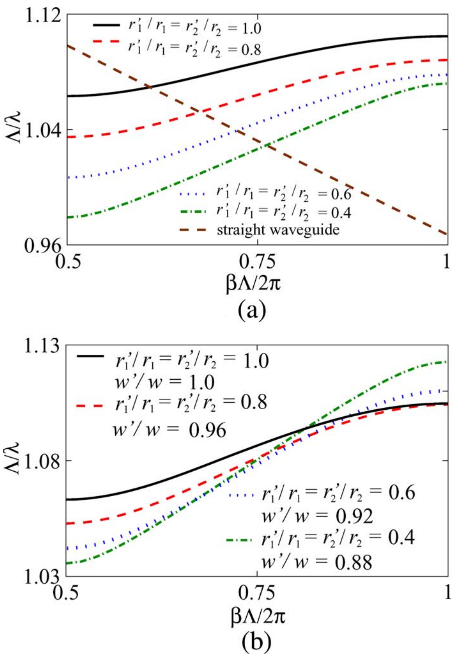

Fig. 5. Dispersion curves of CROWs (a) with different air hole radius and constant waveguide width and (b) with different air hole radius and waveguide widths.

curve is red-shifted as air hole radius decreases. In other words, if we reduce the air hole radius at a constant waveguide width, there is no guided mode at short wavelengths, resulting in the complete suppression of the transmission at short wavelengths as shown in Fig. 4.

In order to adjust the dispersion curve shift due to air hole radius variation, we simultaneously vary the waveguide width and the air hole radius. The dispersion curves for CROWs with different air-hole radius and waveguide width are shown in Fig. 5(b), where the air hole radii r_1 and r_2 are changed to r_1' and r_2', respectively, and the waveguide width w is changed to w'. We can see that the dispersion curve of the CROWs with reduced air hole radius and waveguide width is in the almost same frequency range for the CROWs to be connected with the air hole radii r_1 and r_2 and the waveguide width w. Based on the above analysis, we propose a new tapered structure, type-3, shown in Fig. 6, where the air-hole radius and the waveguide width are changed linearly at the same time. The variation in air-hole radius is defined by (1) whereas, the variation in waveguide width is given as

$$w_{i-1} = w_0 + (w - w_0)(i - 1)/N \tag{3}$$

where w_{i-1} and w_0 are waveguide width at $z = (i-1)\Lambda$ and $z = 0$, respectively. Fig. 7 depicts the transmission characteristic for connection between input waveguide and CROWs using type-3 taper structure with $N = 9$, $R_0 = 0.1$, and $w_0 = 0.82w$. By using the tapered structure type 3, the reflection at the connection end can be minimized and the transmission can be improved drastically. More than 98% transmission is achieved for 42 nm bandwidth around 1550 nm wavelength range in the case of $\Lambda = 1.65$ μm. The total length of the proposed taper is $\sim$ 14.8 μm.

III. Miniaturization of Taper Length

In this section, we consider the effect of waveguide parameters constructing the taper to design more compact tapered structure. At first, we evaluate the effect of R_0. The parameters in previous type-3 structure ($R_0 = 0.1$ and $N = 9$) means that the rate of air hole radius variation $(R_{ij} - R_{(i-1)j})$ is 0.1. Therefore, we can estimate the effect of R_0 by changing type-3 taper for N while keeping $R_{ij} - R_{(i-1)j}$ as 0.1. Fig. 8 shows the transmission characteristics for $R_0 = 0.1, 0.2, 0.3$, and 0.4, where N becomes 9, 8, 7, and 6, respectively. We have to also decide w_0 for each structure, which can be easily determined from the dispersion curves in Fig. 5(b) for fixed R_0 and follows as $0.82w$, $0.84w$, $0.86w$, and $0.88w$, respectively, for each R_0. We can see from Fig. 5 that $R_0 = 0.1$ and 0.2 structures show almost flat top characteristics over 98% transmission, on the other hand, the transmission oscillates as R_0 increases further which is due to the reflection at the connection interface. This is because as N decreases, the waveguide structure approaches to type-1 structure. In case of $R_0 = 0.4$, the transmission oscillates between 0.7 and 1.0, therefore if more than 90% transmission is required, we should keep R_0 less than 0.3. So far, we have considered the tapered structure for constant ratio of air-hole radius variation (0.1). If this value increases, the total taper length decreases, which suggests the decrement of N.

Next, we examine the transmission characteristics for different N while keeping fixed R_0. We have evaluated the transmission characteristics for three values of R_0, namely 0.1, 0.2, and 0.3 and varied the number of periods N in every case. The transmission characteristics are plotted in Figs. 9(a)–(c) for $R_0 = 0.1, 0.2$, and 0.3, respectively, with N as a variable. It can be inferred from the results that the transmission changes abruptly in short wavelengths as we decrease the N, resulting in narrower bandwidth. This may be due to the mismatch of the dispersion relationship between actual tapered structure and the waveguide structure as shown in Fig. 5. The parameters that construct the taper are determined from the dispersion curves for a model structure, where the waveguide width and the air hole radius are varied at a constant rate along z-direction. On the other hand, type-3 taper structure is changed by varying the waveguide width and the air hole radius linearly with a gentle variation in the refractive index, but not with a constant rate. When the rate of air-hole radius variation is small (e.g., $R_{ij} - R_{(i-1)j} = 0.1$), the each sectional taper structure can be approximated by waveguide structure with tailored waveguide width and air hole radius with a constant ratio. However, when the rate of air-hole radius variation becomes large for small N, the taper can not be approximated by the model. This results in mismatch of dispersion relationship and the degradation of transmission at the shorter wavelength range. Also, the waveguide width in taper section changes abruptly for small N structure, therefore scattering loss due to abrupt waveguide width variation should be taken into account. However, more than 99.9% transmission was obtained even for $R_0 = 0.2$ and $N = 2$ structure without air holes (straight waveguide). Hence, scattering loss due to abrupt waveguide width variation is negligible which can be ignored. We can see from Fig. 9 that the taper length can be shortened to less than half of previous type-3 structure with almost same wavelength range by choosing $R_0 = 0.2$ and $N = 4$.

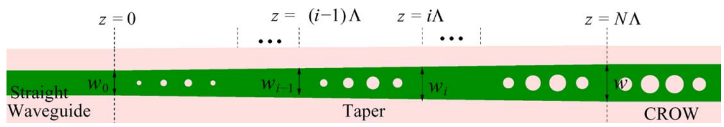

Fig. 6. Connection between 1-D PC-CROW and input straight waveguide using type-3 tapered structure, where the waveguide width and air hole radius are varied linearly at the same time.

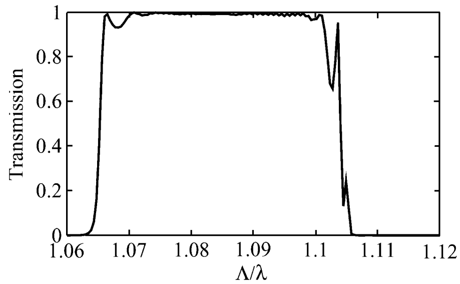

Fig. 7. Transmission characteristics for a type-3 tapered structure.

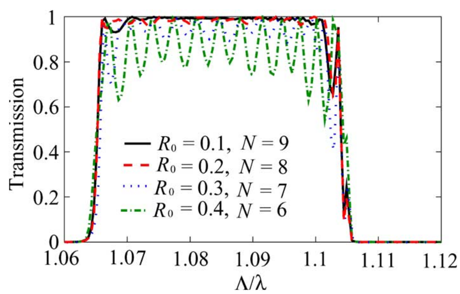

Fig. 8. Transmission characteristics for a type-3 tapered structure with different R_0 at a constant rate of air hole radius variation $(R_{ij} - R_{(i-1)j})$ as 0.1.

IV. Fabrication Tolerance

Here, we consider the fabrication tolerances of taper waveguide. At first, we examine the coupling characteristics of CROWs and straight waveguide by using proposed taper waveguide with error in the air hole radius. We assume that all the air hole in a taper section is fabricated with $\Delta\%$ error from designed parameters. The coupling characteristics can be estimated from dispersion curves, therefore, we show dispersion curves of the 1-D PC-CROWs with various Δ values in Fig. 10(a). In this case, the air hole radius is $r_1'/r_1 = r_2'/r_2 = 0.8 \times (1 + \Delta)$ and the waveguide width is $0.96w$. It is estimated that the value of Δ needs to be controlled within $-5\% < \Delta < 5\%$ range. In Fig. 10(b), we show transmission characteristics for a type-3 tapered structure with $\Delta = 0$, -5%, and 5%. As we have discussed in previous section, R_0, w_0, and N are set as 0.2, $0.84w$, and 4, respectively. We can see that as estimated from dispersion curve, transmission at higher frequency becomes lower for $\Delta = -5\%$ structure, on the other hand at lower frequency, transmission becomes lower for $\Delta = 5\%$ structure. Therefore, air hole radius should be controlled within $\pm 5\%$ error.

Next, we consider the effect of fabrication error in the waveguide width of the taper waveguide. In Fig. 11(a), we show dispersion curves of the 1-D PC-CROWs for $r_1'/r_1 = r_2'/r_2 = 0.8$ and $w'/w = 0.96 \times (1 + \Delta)$. From these results, it is estimated that the waveguide width needs to be controlled within $-5\% < \Delta < 5\%$ range. Fig. 11(b) shows transmission characteristics of type-3 taper structure for $\Delta = 0$, -5%, and 5%. For these Δ value, w_0 becomes $0.84w \times (1 + \Delta)$. In this case, we set R_0 and N as 0.2 and 4, respectively. As estimated from dispersion curve, transmission at the higher frequency becomes lower for $\Delta = 5\%$. We can also see that the bandwidth does not change for $\Delta = -5\%$ structure because these taper structures can support CROW's mode, however, transmission oscillates due to abrupt waveguide width change (refractive index change) in the taper region. This reflection can be reduced by increasing N. For example, we also plot transmission characteristic for $N = 8$ and $\Delta = -5\%$ in Fig. 11(b). We note that increment of N means the number of air hole we have to control increases and taper length becomes longer. If we require more than 90% transmission, w_0 needs to be controlled within $\pm 5\%$ error, ± 20 nm variation. In addition, in a 2-D coupled photonic crystal heterostructure nanocavities, it is known that guiding characteristics are sensitive to waveguide paremeters [27], therefore, the

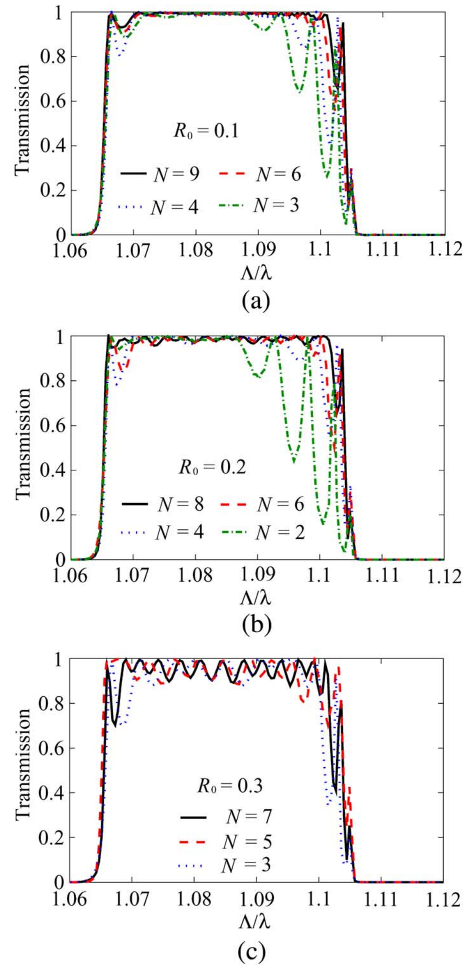

Fig. 9. Transmission characteristics for a type-3 tapered structure for (a) $R_0 = 0.1$, (b) $R_0 = 0.2$, and (c) $R_0 = 0.3$, for different N.

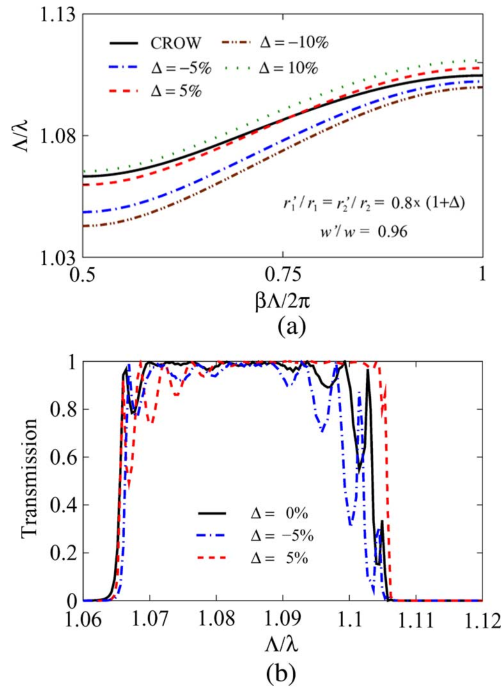

Fig. 10. (a) Dispersion curves and (b) transmission characteritics of CROWs with $\Delta\%$ error in air hole size.

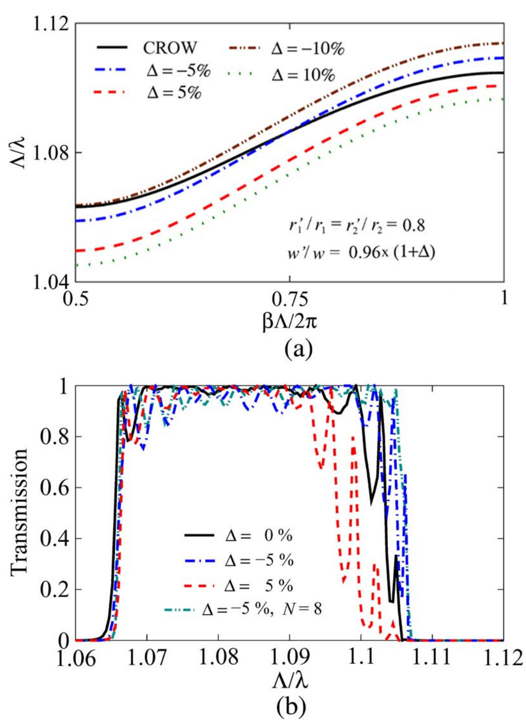

Fig. 11. (a) Dispersion curves and (b) transmission characteritics of CROWs with $\Delta\%$ error in waveguide width.

waveguide parameters of our 1-D PC-CROWs will also need to be well controlled.

Through this investigation, we can see that both air-hole size and waveguide width in the taper waveguide need to be fabricated within $\pm 5\%$ error. Regarding the controllability of the air hole diameters, it is known that the fabrication error can be decreased to the order of 20 nm by using a current fabrication technology relying on the inspection of scanning electron microscope (SEM) images. However, Beggs *et al.* recently proposed a novel measurement technique of the air hole size in photonic crystal slabs and reported that the fabrication error can be reduced to the order of approximately 5 nm [28]. If this technique can be applied to 1-D PC-CROWs, highly efficient coupling will be achieved in the realistically fabricated structure.

V. Conclusion

We have presented a design method of a taper structure for highly efficient connection between 1-D PC-CROWs and straight waveguides. We have first examined the transmission characteristic of a directly connected structure between CROWs and straight waveguides (type 1). Then in order to minimize the effect of reflection at the connection interface, we designed a taper where air hole radius is varied linearly (type 2). These tapers can not achieve efficient connection due to reflection and complete transmission suppression at short wavelengths. The cause of this suppression is the shift of the dispersion curves due to variation in air hole radius. To adjust the dispersion curve shift, we simultaneously varied the waveguide width and the air hole radius and proposed a type-3 tapered structure. The proposed type-3 taper can connect CROWs and straight waveguides with transmission of more than 98% in the whole C-band. Through numerical simulations, we find a 14.8 μm taper length which can be further reduced by varying R_0 and N to a value of 6.6 μm for a suitable set of R_0 and N. We have also shown fabrication tolerances of the taper waveguide and found that both the air hole and waveguide width need to be controlled within $\pm 5\%$ fabrication error.

In order to consider the scattering losses in the vertical direction, one has to carry out 3-D simulations, which are currently under consideration.

References

[1] Y. Xu, R. K. Lee, and A. Yariv, "Propagation and second-harmonic generation of electromagnetic waves in a coupled-resonator optical waveguide," *J. Opt. Soc. Amer. B*, vol. 17, pp. 387–400, Mar. 2000.

[2] W. J. Kim, W. Kuang, and J. O'Brien, "Dispersion characteristics of photonic crystal coupled resonator optical waveguides," *Opt. Express*, vol. 11, pp. 3431–3437, Dec. 2003.

[3] T. Sakamoto, A. Okada, M. Hirayama, Y. Sasaki, O. Moriwaki, I. Ogawa, R. Sato, K. Noguchi, and M. Matsuoka, "Optical packet synchronizer using wavelength and space switching," *IEEE Photon. Technol. Lett.*, vol. 14, no. 9, pp. 1360–1362, Sep. 2002.

[4] H. J. S. Dorren, M. T. Hill, Y. Liu, N. Calabretta, A. Srivatsa, F. M. Huijskens, H. de Waardt, and G. D. Khoe, "Optical packet switching and buffering by using all-optical signal processing methods," *J. Lightwave Technol.*, vol. 21, no. 1, pp. 2–12, Jan. 2003.

[5] R. S. Tucker, P. C. Ku, and C. J. C. Hasnain, "Slow-light optical buffers: Capabilities and fundamental limitations," *J. Lightwave Technol.*, vol. 23, no. 12, pp. 4046–4066, Dec. 2005.

[6] T. Otani, T. Miyazaki, and S. Yamamoto, "40-Gb/s optical 3R regenerator using electroabsorption modulators for optical networks," *J. Lightwave Technol.*, vol. 20, no. 2, pp. 195–200, Feb. 2002.

[7] J. Leuthold, P. A. Besse, E. Gamper, M. Dulk, S. Fischer, G. Guekos, and H. Melchior, "All-optical Mach-Zender interferometer wavelength converters and switches with integrated data- and control- signal separation scheme," *J. Lightwave Technol.*, vol. 17, no. 6, pp. 1056–1066, Jun. 1999.

[8] J. Company, J. Cascon, D. Peter, and B. Ortega, “Reconfigurable fiber-optic delay line filters incorporating electrooptic and electroabsorption modulators,” *IEEE Photon. Technol., Lett.*, vol. 11, no. 9, pp. 1174–1176, Sep. 1999.

[9] N. Stefanou and A. Modinos, “Impurity bands in photonic insulators,” *Phys. Rev. B*, vol. 57, pp. 12127–12133, May 1998.

[10] A. Yariv, Y. Xu, R. K. Lee, and A. Scherer, “Coupled-resonator optical waveguide: A proposal and analysis,” *Opt. Lett.*, vol. 24, pp. 711–713, Jun. 1999.

[11] M. Bayindit, B. Temelkuran, and E. Ozbay, “Propagation of photons by hopping: A waveguiding mechanism through localized coupled cavities in three-dimensional photonic crystals,” *Phys. Rev. B*, vol. 61, pp. R11855–R11857, May 2000.

[12] S. Oliver, C. Smith, M. Rattier, H. Benisty, C. Weisbuch, T. Krauss, R. Houdre, and U. Oesterle, “Miniband transmission in a photonic crystal coupled-resonator optical waveguide,” *Opt. Lett.*, vol. 26, pp. 1019–1021, Jul. 2001.

[13] S. Lan, S. Nishikawa, H. Ishikawa, and O. Wada, “Engineering photonic crystal impurity bands for waveguides, all-optical switches and optical delay lines,” *IEICE Trans. Electron.*, vol. E85-C, pp. 181–189, Jan. 2002.

[14] S. Mookherjea and A. Yariv, “Coupled-resonator optical waveguides,” *IEEE J. Sel. Top. Quantum Electron.*, vol. 8, no. 5, pp. 448–456, May 2002.

[15] T. J. Karle, D. H. Brown, R. Wilson, M. Steer, and T. F. Krauss, “Planar photonic crystal coupled cavity waveguides,” *IEEE J. Sel. Top. Quantum Electron.*, vol. 8, no. 8, pp. 909–918, Aug. 2002.

[16] T. J. Karle, Y. J. Chai, C. N. Morgan, I. H. White, and T. F. Krauss, “Observation of pulse compression in photonic crystal coupled cavity waveguides,” *J. Lightwave Technol.*, vol. 22, no. 2, pp. 514–519, Feb. 2004.

[17] J. K. S. Poon, J. Scheuer, Y. Xu, and A. Yariv, “Designing coupled-resonator optical waveguide delay lines,” *J. Opt. Soc. Amer. B*, vol. 21, pp. 1665–1673, Sep. 2004.

[18] J. K. Poon, L. Zhu, G. A. Derose, and A. Yariv, “Transmission and group delay of microring coupled-resonator optical waveguides,” *Opt. Lett.*, vol. 31, pp. 456–458, Feb. 2006.

[19] F. Xia, L. Sekaric, M. O’Boyle, and Y. Vlasov, “Coupled resonator optical waveguides based on silicon-on-insulator photonic wires,” *Appl. Phys. Lett.*, vol. 89, pp. 041122–041124, Jul. 2006.

[20] M. L. Povinelli and S. Fan, “Radiation loss of coupled-resonator optical waveguides in photonic-crystal slabs,” *Appl. Phys. Lett.*, vol. 89, pp. 191114–191116, Nov. 2006.

[21] Y. Sugimoto, S. Lan, S. Nishikawa, N. Ikeda, H. Ishikawa, and K. Asakawa, “Design and fabrication of impurity band-based photonic crystal waveguides for optical delay lines,” *Appl. Phys. Lett.*, vol. 81, pp. 1946–1948, Sep. 2002.

[22] S. Nishikawa, S. Lan, N. Ikeda, Y. Sugimoto, H. Ishikawa, and K. Asakawa, “Optical characterization of photonic crystal delay lines based on one-dimensional coupled defects,” *Opt. Lett.*, vol. 27, pp. 2079–2081, Dec. 2002.

[23] A. Martinez, J. Garcia, P. Sanchis, F. C. Soto, J. Blasco, and J. Marti, “Intrinsic losses of coupled-cavity waveguides in planar-photonic crystals,” *Opt. Lett.*, vol. 32, pp. 635–637, Mar. 2007.

[24] Y. Kawaguchi, N. Kono, K. Saitoh, and M. Koshiba, “Loss reduction mechanism for coupled cavity waveguides in one-dimensional photonic crystals,” *J. Lightwave Technol.*, vol. 26, no. 10, pp. 3461–3467, Oct. 2008.

[25] A. R. M. Zain, N. P. Johnson, M. Sorel, and R. M. De La Rue, “Ultra high quality factor one dimensional photonic crystal/photonic wire micro-cavities in silicon-on-insulator (SOI),” *Opt. Express*, vol. 16, pp. 12084–12089, Aug. 2008.

[26] M. Koshiba, Y. Tsuji, and M. Hikari, “Time-domain beam propagation method and its application to photonic crystal circuits,” *J. Lightwave Technol.*, vol. 18, no. 1, pp. 102–110, Jan. 2000.

[27] D. O’Brien, M. D. Settle, T. Karle, A. Michaell, M. Salib, and T. F. Krauss, “Coupled photonic crystal heterostruture nanocavities,” *Opt. Express*, vol. 15, pp. 1228–1233, Jan. 2007.

[28] D. M. Beggs, L. O’Faolain, and T. F. Krauss, “Accurate determination of the functional hole size in photonic crystal slabs using optical methods,” *Photon. Nanostructures*, vol. 6, pp. 213–218, Oct. 2008.

Yuki Kawaguchi was born in Hokkaido, Japan, on November 15, 1983. He received the B.S. degree in electronic engineering and the M.S. degree in media and network technologies from Hokkaido University, Sapporo, Japan, in 2007 and 2009, respectively, where he is currently working toward the Ph.D. degree in information science.

He has been a Research Fellow of the Japan Society for the Promotion of Science since 2009. He has been engaged in research on modeling of photonic integrated circuit using finite element method.

Mr. Kawaguchi is a member of the Institute of Electronics, Information and Communication Engineers (IEICE) of Japan.

Kunimasa Saitoh (S’00–M’01) was born in Hokkaido, Japan. He received the B.S., M.S., and Ph.D. degrees in electronic engineering from Hokkaido University, Sapporo, Japan, in 1997, 1999, and 2001, respectively.

From 1999 to 2001, he was a Research Fellow of the Japan Society for the Promotion of Science. From 2001 to 2005, he was a Research Associate of Graduate School of Engineering at Hokkaido University. In 2005, he became an Associate Professor with the Graduate School of Information Science and Technology, Hokkaido University. He has been engaged in research on fiber optics, nano-photonics, integrated optical devices, and computer-aided design and modeling of guided-wave devices using finite element method, beam propagation method, and so on. He is an author or coauthor of more than 100 research papers in refereed international journals.

Prof. Saitoh is a member of the Institute of Electronics, Information, and Communication Engineers (IEICE) and the Optical Society of America (OSA). In 1999 and 2002, he was awarded the Excellent Paper Award and the Young Scientist Award from the IEICE, respectively, and in 2008, the Young Scientists’ Prize of the Commendation for Science and Technology from the Ministry of Education, Culture, Sports, Science, and Technology (MEXT), Government of Japan.

Masanori Koshiba (M’76–SM’87–F’03) was born in Sapporo, Japan. He received the B.S., M.S., and Ph.D. degrees in electronic engineering from Hokkaido University, Sapporo, Japan, in 1971, 1973, and 1976, respectively.

In 1976, he joined the Department of Electronic Engineering, Kitami Institute of Technology, Kitami, Japan. From 1979 to 1987, he was an Associate Professor of Electronic Engineering at Hokkaido University, and in 1987, he became a Professor there. He has been engaged in research on wave electronics, including microwaves, millimeter-waves, lightwaves, surface acoustic waves (SAW), magnetostatic waves (MSW), and electron waves, and computer-aided design and modeling of guided-wave devices using finite element method, boundary element method, beam propagation method, and so on. He is an author or coauthor of more than 300 research papers in refereed international journals. He is an author of the books *Optical Waveguide Analysis* (McGraw-Hill, 1992) and *Optical Waveguide Theory by the Finite Element Method* (Kluwer Academic, 1992), and is a coauthor of the books *Analysis Methods for Electromagnetic Wave Problems* (Artech House, 1990), *Analysis Methods for Electromagnetic Wave Problems, Vol. Two* (Artech House, 1996), *Ultrafast and Ultra-Parallel Optoelectronics* (Wiley, 1995), and *Finite Element Software for Microwave Engineering* (Wiley, 1996).

Prof. Koshiba is a fellow of the Institute of Electronics, Information, and Communication Engineers (IEICE), and is a member of the Institute of Electrical Engineers of Japan, and the Institute of Image Information and Television Engineers of Japan. In 1987, 1997, and 1999, he was awarded the Excellent Paper Awards from the IEICE, in 1998, the Electronics Award from the IEICE-Electronics Society, and in 2004, the Achievement Award from the IEICE. From 1999 to 2000, he served as a President of the IEICE-Electronics Society, and in 2002, he served as a Chair of the IEEE LEOS (Lasers and Electro-Optics Society) Japan Chapter. Since 2003, he has served on the Board of Directors of the IEICE.